INVITED PAPER

Ocean and Geothermal Energy Systems

This paper discusses different forms of ocean energy along with land-based ocean energy. The comparative costs and grid interface issues are discussed.

By Annette von Jouanne, *Fellow IEEE*, and Ted K. A. Brekken, *Senior Member IEEE*

ABSTRACT | This paper presents techno-economic summaries of ocean wave, tidal and current, ocean thermal, and geothermal energy, including grid interface characteristics. These forms of energy represent a significant opportunity to complement diversified energy conversion portfolios. Ocean wave energy conversion relies on the capture of kinetic and potential energy in moving and elevated water in an ocean wave. Tidal and current technology converts the kinetic energy in moving water, much like a wind turbine. Ocean thermal converts the energy available in the temperature gradient of warm surface water and cold deep water. Last, geothermal conversion utilizes the hot rock and water deep within the Earth. The total global average wave resource is estimated at approximately 2000 GW, with approximately 300 GW in the United States. The total global tidal resource is estimated at approximately 1000 GW, with 50 GW in the United States. The marine current resource estimate for the Florida Current in the southeast United States is estimated at 5 GW. Ocean thermal has a global capacity estimate of 5000 GW. Last, the global conventional hydrothermal geothermal capacity estimate is approximately 200 GW, but with much more possible through enhanced geothermal systems. For cost, it was found that the long-term projected wave energy conversion cost is \$0.10–\$0.15/kWh. The long-term projected tidal cost is found to be \$0.025–\$0.25/kWh. Ocean thermal long-term cost is projected at \$0.10–\$0.18/kWh. And last, geothermal, being more closely aligned with traditional thermal generation, is estimated at \$0.03/kWh to \$0.15/kWh.

KEYWORDS | Costs; geothermal energy; oceanic engineering and marine technology; renewable energy sources; wave power

Manuscript received January 17, 2017; revised April 24, 2017; accepted April 25, 2017. Date of publication August 11, 2017; date of current version October 18, 2017.
(Corresponding author: Ted K. A. Brekken.)
A. von Jouanne is with Baylor University, Waco, TX 76708 USA (e-mail: Annette_vonJouanne@Baylor.edu)
T. Brekken is with Oregon State University, Corvallis, OR 97331 USA (e-mail: brekken@eecs.oregonstate.edu).

Digital Object Identifier: 10.1109/JPROC.2017.2699558

I. INTRODUCTION

Ocean energy and geothermal energy represent a significant renewable energy resource. Ocean energy exists in several different forms, including potential and kinetic energy in waves, tidal and ocean currents, heat gradients, and salinity gradients. All of these forms, including geothermal, are renewable. Ocean energy from waves, currents, and ocean thermal is essentially different forms of solar energy, while tidal energy is from the Earth–moon gravitational interaction. Geothermal energy primarily comes from radioactive decay deep within the Earth and residual heat from the formation of the Earth [1].

Ocean wave energy is the energy in potential and kinetic energy of moving and elevated water within a wave. Tidal and current energy is the kinetic energy in moving water, such as a stream or tidal inlet. Ocean thermal energy is the energy recoverable in the temperature gradient between warm surface water and cold deep water. Geothermal energy is completely separate from ocean energy, and is the energy available in hot rock and water deep underground. This paper presents techno–economic summaries of these forms of energy, including information on the conversion technology and power electronics approach as applicable.

II. WAVE

A. Resource Characteristics

Uneven heating of the surface of the Earth drives wind, and wind across water creates waves. At each stage of energy conversion from solar to wind to wave the power density increases. For ocean wave power, the density is on the order of tens of kilowatts per meter of wave front (transverse to the direction of wave propagation). This high power-density along with good forecastability and lower variability—compared to solar and wind [2]—make ocean wave power an attractive resource.

Waves are created by a combination of factors, but dominant among them for deep-water waves is the creation of a

pressure differential across the crest and trough caused by air flowing over the wave. As the air moves over the crest of a wave, it accelerates, causing relatively lower pressure at the crest then at the trough, where the air is moving more slowly.

The waves created by this process experience very little damping or friction in deep water, thus they propagate with very little loss across the ocean, becoming larger and larger as they experience wind systems along their journey. Global winds around 30 ° latitude to 45 ° latitude—the Westerlies—blow from west to east. These winds create large wave systems that travel west to east across the oceans, making landfall on the west coasts of continents, generally stronger the further the latitude is away from the equator.

The transfer of energy from the air to the water causes the water molecules to move and to elevate. Thus, ocean wave energy exists as kinetic and potential energy in water molecules transferred one to the other as a wave propagates. The energy moves at the wave group velocity, which for large ocean swells in deep water is typically on the order of 5–10 m/s. This relatively slow propagation of energy, combined with very low energy loss, is one reason why wave power generally has good forecastability [3].

Wave power is calculated by multiplying the wave energy by the group velocity, and is typically 30 kW/m of wave front (transverse to the wave propagation direction) and higher for a good wave power site (e.g., the West Coast of the United States). The equation for wave power is

$$P = \frac{\rho g^2}{64\pi} H_s^2 T_e \left[\frac{W}{m}\right] \quad (1)$$

where P is the wave power per meter of wave front (transverse to the direction of wave propagation), ρ is water density, g is the acceleration of gravity, H_s is the significant wave height, and T_e is the energy period [4]. Note that the power is proportional to wave period, and proportional to the square of the wave height.

Fig. 1 shows the ocean power per meter for the United States. It is noted that the resource is much larger on the West Coast than the East Coast, and that the resource generally increases from south to north.

The wave climate power is characterized by two factors: wave height and period. (In contrast to wind or solar in which the resource is largely characterized only by wind speed and irradiance, respectively.)

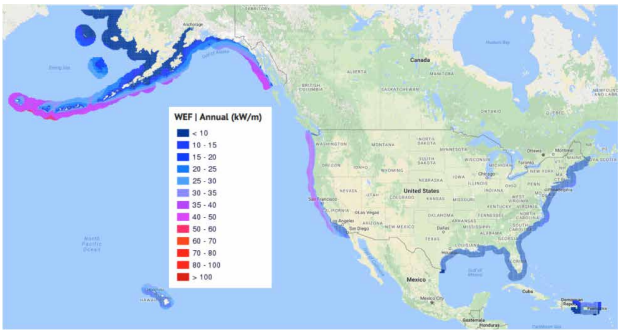

Fig. 1. *Annual wave energy per meter for the United States (from the NREL MHK Atlas, online).*

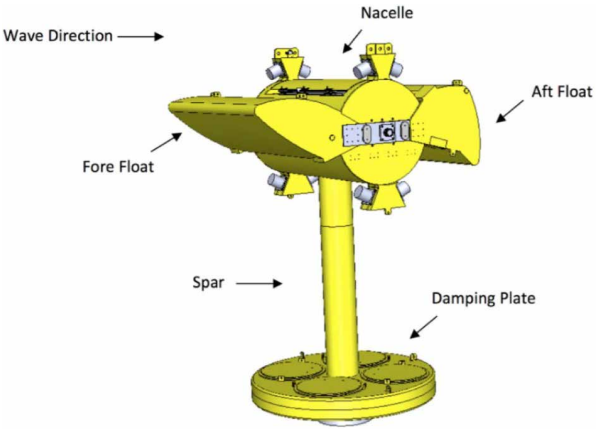

Fig. 2. *Columbia Power Technologies SeaRay [9].*

The total available wave energy resource along the U.S. West Coast (including Alaska) is estimated to be 2640 TWh/yr (301 GW average). Assuming 15 MW of rated generation per kilometer, the total recoverable wave energy resource is 1170 TWh/yr [5]. Comparing to an estimated 3897 TWh of electrical energy supplied to the grid in 2015 [6], that is approximately 25% of the U.S. electrical needs. The global total average wave power estimate is over 2000 GW [7].

B. Wave Energy Conversion Technologies

There are several ways of categorizing wave energy converters (WECs) [8]. Here we present three broad categories: oscillating body, oscillating water column, and overtopping.

Oscillating bodies operate on the simple premise that the pressure of an ocean wave drives a body to move in a cyclical fashion relative to a fixed point (such as a mooring) or another body.

Fig. 3. *Ocean Power Technologies PB3 PowerBuoy deployed off the coast of New Jersey. (Image courtesy of Ocean Power Technologies.)*

Fig. 4. *Weptos WEC. (Image courtesy of Weptos.)*

This motion can be in any of six degrees of freedom—heave, surge, pitch, roll, yaw, and sway—although heave, surge, or pitch are the most typically exploited for wave energy. Conversion of the energy is typically achieved by placing an electromagnetic or hydraulic mechanism between the oscillating body and the fixed point, or in the case of multiple bodies, between the bodies.

Examples of oscillating bodies include the SeaRay from Columbia Power Technologies, the Powerbouy from Ocean Power Technologies, the Weptos WEC, and the NWEI (Northwest Energy Innovations) Azura (Figs. 2–5).

The second category is the oscillating water column (OWC). OWC devices use the oscillating pressure wave from the ocean to cyclically pressurize the air trapped in an enclosed chamber [10]. This pressurized air is released through a narrow aperture in the chamber to drive an air turbine. Examples of this technology include the Limpet (one of the oldest grid connected projects), the Mutriku wave power plant in Spain, a 500-kW OWC at Jeju island in Korea, the Oceanlinx series of wave energy converters, and the Ocean Energy OWC (Figs. 6–8).

The third category is overtopping, in which a ramp or narrowed channel causes the water near the crest of a wave to spill over a retaining wall and fill a basin. This effectively creates a low-head hydro resource, and the energy is converted by running the basin water out through a low-head hydro turbine. Some of the earliest and largest projects have been of this type, including the Tapchan project in Norway and the Danish Wave Dragon project (Fig. 9) [12].

Fig. 5. *Northwest Energy Innovations (NWEI) Azura. (Image courtesy of NWEI.)*

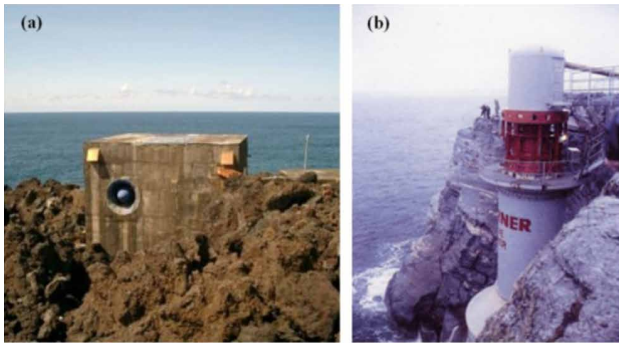

Fig. 6. *(a) Pico OWC. (b) Demonstration plant at Toftestallen [11].*

C. Power Electronics and Control

Due to the limited number of grid connected wave energy projects to date, there is not a large body of experience for power electronic conversion of ocean wave power in the field. However, some general observations and requirements can be surmised. An overview of some of the most common conversion strategies is shown in Fig. 10.

In the field of ocean wave energy, the physical mechanism that converts the wave energy to another useful form (typically electrical energy), is called the power takeoff (PTO).

Wave energy converter control, i.e., control of the force and velocity of the PTO, is a complex topic. There are several linear and nonlinear approaches that have received significant attention [15], [16]. The type of control that can be applied also depends on the type of PTO used.

For oscillating body type converters, an electrical machine connected directly between the bodies will oscillate in both negative and positive directions of rotation. If this machine is a synchronous type, with the field supplied by permanent magnets or a field winding, the oscillating position, speed, and acceleration will create a frequency and amplitude modulated back-EMF. This can be managed via rectification of the generator electrical output via a diode-bridge to a direct current (dc) link. An inverter can then couple the dc link to the alternating current (ac) mains [17]–[19]. The advantage of this design is simplicity, however, control over the generator torque is generally imprecise—limited to controlling the

Fig. 7. *Oceanlinx MK1 full scale prototype [11].*

Fig. 8. ***Wavegen Mutriku breakwater [11].***

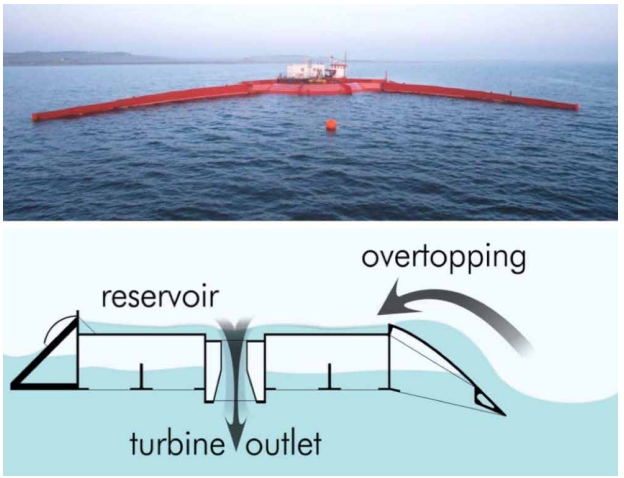

Fig. 9. ***Wave Dragon overtopping WEC [13].***

dc link voltage to control the generator RMS current—and power quality of current in the generator will be poor. Another option is to use an ac–ac converter (e.g., a matrix converter or back-to-back inverters) to couple the variable generator output to the ac mains [20]–[23]. This is more complex, but affords greater precision and control, particularly the ability to motor the wave energy converter, which is momentarily required in some cases of optimal control [16].

Example waveforms for a directly connected linear generator are shown in Fig. 11.

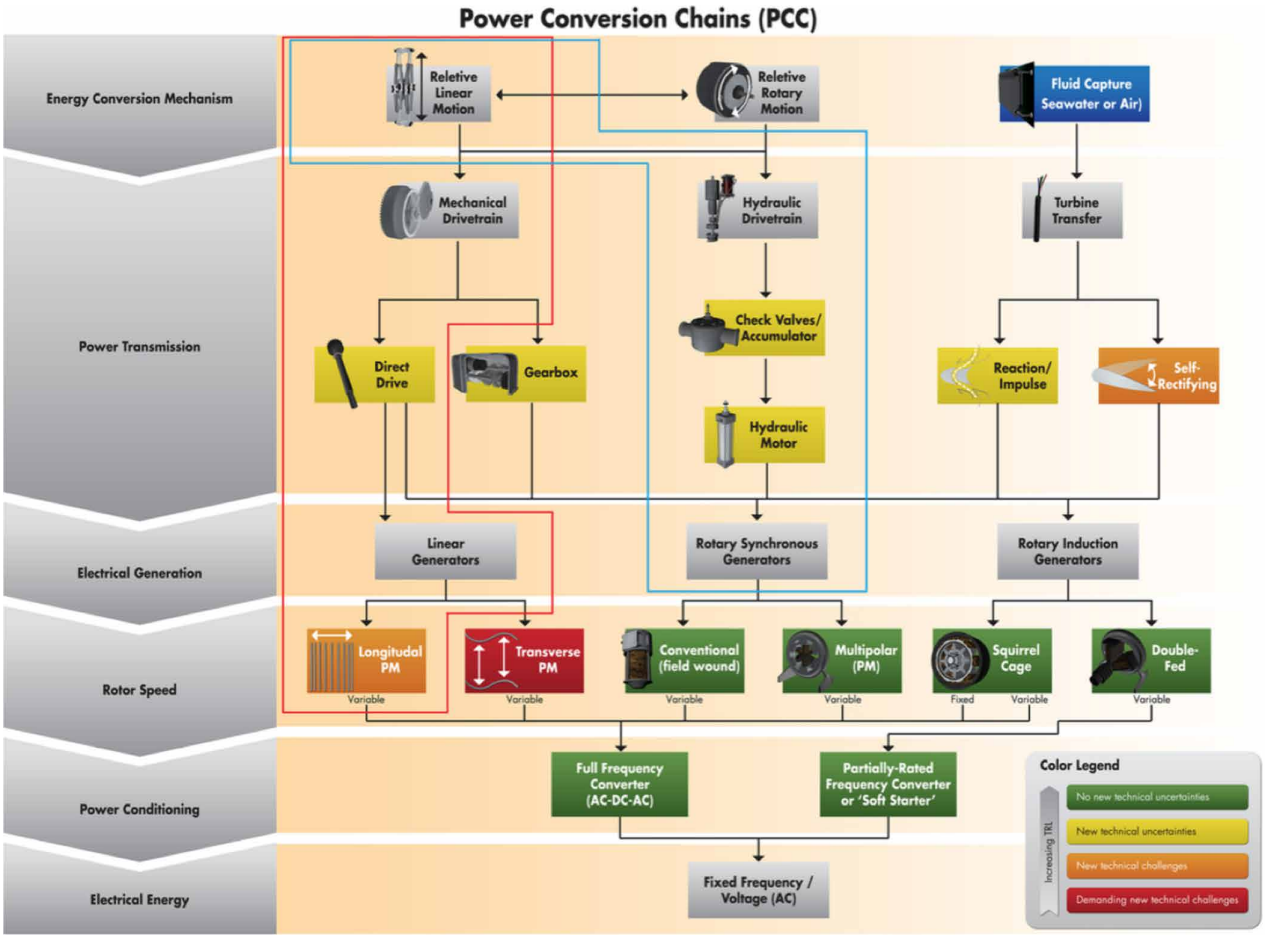

Fig. 10. ***Wave energy conversion strategies [14]. Linear motion can be converted to rotary motion (or vice versa) via belt or chain drives, rack and pinions, sliding screw systems, or crank shaft systems. The blue outline box contains typical components of a hydraulic system, and the red outline box contains typical components of a direct-drive electromagnetic system.***

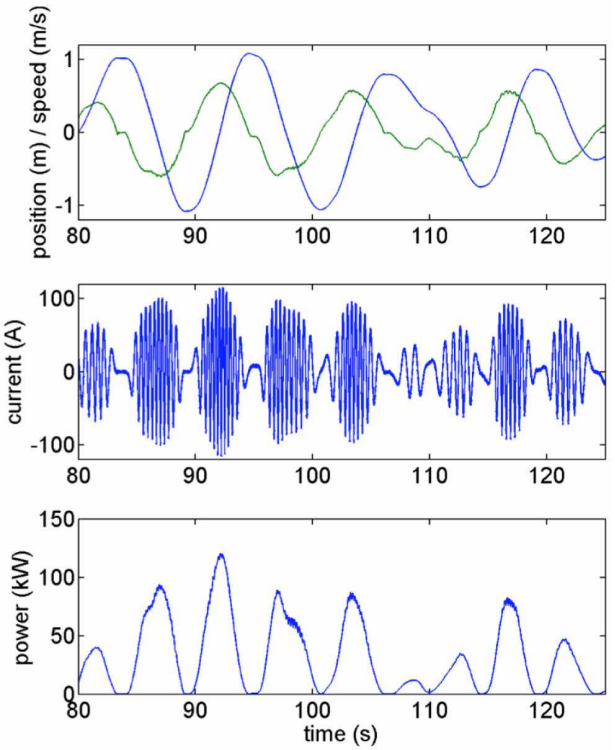

Fig. 11. *Example direct-drive wave energy converter waveforms [13].*

Here it can be seen that current produced by the machine, before being processed by the power electronics for grid connection, is both frequency and amplitude modulated in accordance with the machine speed, and that the power produced varies with the ocean wave excitation with a periodic behavior of approximately 5 s.

In some cases for oscillating body type converters a hydraulic machine is used as the main PTO, with an electrical generator connected to the hydraulic machine. In that case check valves are often used to rectify the hydraulic fluid and thus allow for unidirectional rotation of the electrical generator. This allows the use of grid-connected induction generators, very similar in application to early wind turbines [24]. (Though it is noted that directly connected induction generators have poor fault characteristics, and are not encouraged by modern standards [25].)

Electrical standards for ocean wave energy are IEC/TS 62600-100, which covers measurement of power and energy and determination of WEC power curves and mean annual energy production, and IEEE Std 1547 "Standards for Interconnecting Distributed Resources with Electric Power Systems," which largely covers interconnection standards. The unique oscillating operation of a directly connected electric machine also requires careful rating and consideration, and is not explicitly covered in current standards [26], [27].

Power quality issues—such as harmonics, flicker, and fault ride through—are much the same as any generator with a full-rated power electronics connection to the grid (e.g., some wind turbine designs) [13], [21]–[23], [28]–[31]. In fact, it is anticipated that many of the standards, issues, and concerns applicable to wind energy converters are the best starting place for ocean wave energy conversion technologies [25].

It is expected that geographical diversity and energy storage will play an important role for wave energy. It has been shown that geographic diversity (i.e., placing the individual WECs of an array such that they do not produce maximums or minimums of power at the same time) has an important impact on short timescale variability of the power output [25], [32]–[34].

Last, like many nondispatchable, variable power sources, the variability of wave power on the seconds, minutes, or hours timescale raises concerns for grid stability and the ability to provide reserves. Studies have generally found that the integration of wave power is similar in impact to the integration of wind power [2], [34]–[38].

D. Autonomous Applications

The majority of the focus of this paper is on grid-connected technologies for bulk electricity generation, but there is a significant market for autonomous, off-grid applications. For example, powering sensors and communication equipment on data buoys, or providing power for open ocean or island vessels and bases. In fact, one of the very first applications of ocean wave energy was for Japanese naval navigation buoys, configured as small oscillating water columns by the naval officer Yoshio Masuda, eventually reaching commercialization in 1965 [39]. Many current WEC developers are looking into adapting their large-scale devices for these small autonomous applications as well.

E. Cost

Sixteen studies on wave energy cost conducted in the United States, Europe, and Australia are summarized in Fig. 12 [25].

The data are adapted from [25]. The median COE from the 16 studies is \$0.24/kWh. This puts the current price of wave energy several times higher than grid competitiveness, which would typically be in the range of \$0.05/kWh to \$0.10/kWh. The capital cost of power capacity is shown in Fig. 13. Of the six studies, the median is \$3.28/W. This is generally three to four times higher than the grid-competitiveness benchmark of \$1/W.

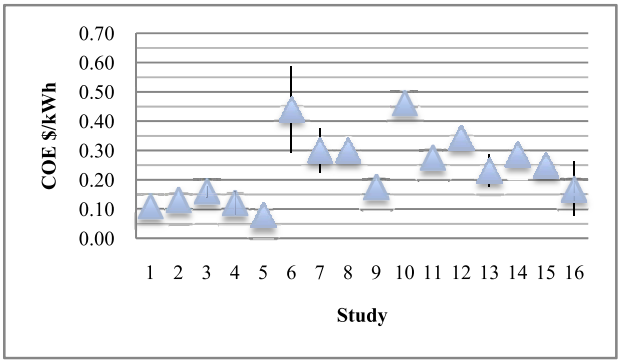

Fig. 12. *The total median COE is \$0.24/kWh. (Data adapted from [25].)*

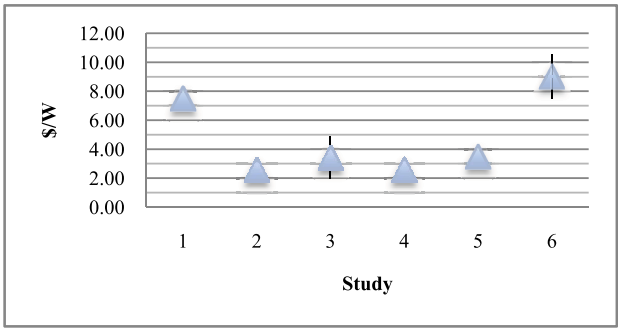

Fig. 13. *Median cost of power is $3.28/W. (Data adapted from [25].)*

Other studies based on surveys of ocean wave energy developers as well as published results from prototypes and early deployments suggest that the capital expenses for large-scale ocean deployments (i.e., 10–100 MW) converge to approximately $5/W [40].

The overall cost of energy depends on anticipated reductions in cost as the industry accumulates total installed capacity worldwide. Chozas [40] studied Levelized Cost of Energy as a function of penetration and found "The curves show that in the long term, after more than 10 GW of capacity are deployed, wave energy could reach $100–$150/MWh, or even lower in the more optimistic estimates" [40].

III. OCEAN THERMAL ENERGY CONVERSION (OTEC)

Ocean thermal energy conversion (OTEC) is a marine renewable energy process that produces power by using the temperature differential between the water layers of the warm ocean surface and the deep cold ocean of about 800–1000 m [41]. Solar energy is stored as heat within the ocean surface layer and mixed by wave motion to water depths of about 100 m. The deeper ocean consists of colder water, where the thermocline, or transition layer, between the warmer surface water and the cooler deep water is sometimes marked by an abrupt change in temperature, but more often the change is gradual [42]. Thus, the ocean offers a combustion free heat source and the heat sink required for a heat engine.

OTEC plants can be either land based (see Fig. 14) or floating infrastructures to enable economic access to the required warm and cold seawater resources. In OTEC technologies, warm surface seawater is used to cause flash evaporation of either the seawater itself or of a low boiling point working fluid such as ammonia, where the expanding vapor drives a turbine generator. Cold deep seawater pumped through a heat exchanger condenses the vapor back into a liquid and ensures the pressure differential to drive the turbine [43]. OTEC has the potential to be a favored baseload renewable resource in that it is dispatchable and able to provide around-the-clock generation and balancing of variable renewables with capacity factors ranging from 90% to 95% [43].

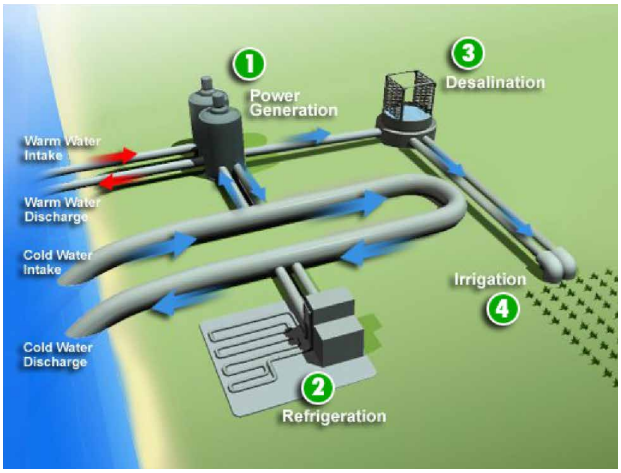

Fig. 14. *Diagram of a land-based OTEC plant. (Image courtesy of the Ocean Thermal Energy Corporation.)*

In addition to generating electricity through OTEC technologies, the ocean thermal resource has other applications including the production of freshwater and the production of energy-intensive products such hydrogen, oxygen, and ammonia through electrolysis [42]. OTEC technologies also support industries such as marine aquaculture using the nutrient rich cold water brought to the surface, as well as chilled-soil agriculture (which allows for the cultivation of temperate-zone plants in tropical environments) and using the cold deep water as the chiller fluid in air conditioning systems [41]–[47]. Seawater air conditioning systems use cold seawater rather than a compressor-chilled working fluid as the heat sink for air conditioning heat exchangers and other refrigeration applications. Large data centers could also benefit from both the equipment cooling and power generation provided by OTEC [47]. A diagram of a land-based OTEC system is shown in Fig. 14, depicting the warm and cold seawater intakes and returns, power generation (1), as well as coproducts of refrigeration and seawater air conditioning (2), desalinated water (3), and agricultural irrigation (4). Power generation will be the focus of the remainder of this OTEC section.

The requirements for OTEC to be a renewable energy resource include continued warming of the ocean surface by the sun, and the availability of cold ocean water at depth. Cold deep seawater is produced through thermohaline circulation of ocean waters driven by natural density gradients due to salinity, surface heat, and freshwater influxes in different parts of the ocean [42]. The global power resource that could be extracted with OTEC plants without affecting the thermohaline ocean circulation is estimated to be at least 5000 GW, e.g., 10 000 × 500 MW OTEC plants [48]. Put in perspective, this would be about twice the amount of power projected for worldwide electricity consumption by 2025 [42].

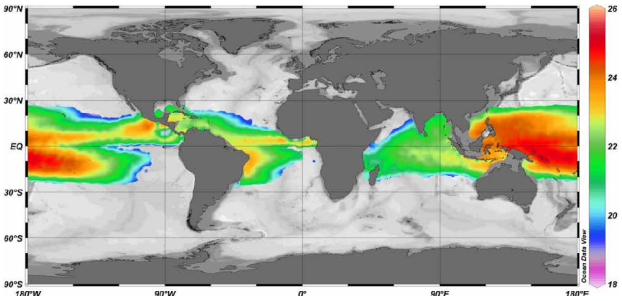

Fig. 15. *Average ocean temperature differentials ΔT between 20- and 1000-m water depths, using WOA05 data with a color palette from 18 °C to 26 °C. (Image courtesy of [49].)*

A. Resource Characteristics

The ocean thermal resource is defined by ΔT, the temperature differential between water depths of 20 and 1000 m [42]. Worldwide, ΔT typically ranges from 10 °C to 25 °C, with the higher values found in tropical waters closer to the equator [41]. For efficient power production, a ΔT of at least 20 °C within 1000 m below the ocean surface is preferred [44], [47]. At 1000-m water depths, temperatures are relatively constant at about 4 °C–5 °C [47]. Thus, with a relatively constant temperature of 4 °C at 1000 m, ΔT is driven by surface temperatures, where OTEC is particularly suitable for average surface temperatures around 25 °C [43].

Fig. 15 shows a map of the average OTEC thermal resource ΔT using World Ocean Atlas 2005 (WOA05) data [49]. Considering the important criteria of ΔT and feasible access to deep water, Fig. 15 sheds light on favorable OTEC sites. For example, the Hawaiian Archipelago is very well located from both a thermal resource perspective, and due to the fact that volcanic islands have a steep bathymetry (seafloor topography), enabling expedient access to deep water. Global estimates of the extractable net power from OTEC total 6300 GW [47], while as stated above, the power extraction estimate to prevent affecting the thermohaline circulation is at least 5000 GW [48]. From [47], over 500 GW is available from within U.S. waters.

B. OTEC Technologies

While OTEC technologies have existed for decades, with the first electricity-producing OTEC plant built in 1930 in Cuba rated at 22 kW, commercial adoption has been slow [46], due to high capital costs and the lack of experience building OTEC plants at scale [43], [47]. Research is continuing on optimized plant designs and multiuse market applications including desalination of seawater, cooling of buildings, and use of cold water in aquaculture applications [46]. The two primary OTEC technologies are differentiated by the working fluids used. Open-cycle OTEC (OC-OTEC) technologies use seawater as the working fluid, whereas closed-cycle OTEC (CC-OTEC) commonly uses ammonia, with a low-temperature evaporation point, as the working fluid. Both OC- and CC-OTEC technologies can be either land based or floating infrastructures. Land-based systems are considered a niche market, needing 1000-m depth close to shore [42], and could face more stringent permitting challenges associated with the siting of the large seawater pipes. The primary candidate for commercial size plants appears to be the floating OTEC plant, positioned close to land, transmitting power to shore via a submarine power cable [42]. OC-OTEC systems offer the benefit of producing freshwater as a byproduct, while they also require larger turbine diameters [42]. The OTEC system efficiency, based on the thermal resource, is affected by several parameters including the power plant design and the matching with the seawater components, plant size, and the resource temperatures. Theoretical maximum Carnot cycle efficiencies of heat engines depend on the temperature differentials, and for a 20 °C ΔT OTEC system, the maximum efficiency is 7% [50]. The overall efficiency, based on ΔT, would be further reduced to about 3%–5% in practical OTEC installations due to inherent pumping loads and component losses within the system [51], [52]. While efficiency is an important driver in utilizing resources, better assessments for renewable technologies include the levelized cost of energy (LCOE) and environmental impacts in comparison with other available resources.

C. Open-Cycle OTEC

For open-cycle OTEC (OC-OTEC) the working fluid is warm surface seawater which is injected into a vacuum chamber, where the pressure is reduced below the saturation value corresponding to its temperature causing flash evaporation. The resulting low-pressure steam expands to drive a turbine generator. Fig. 16 depicts the steps of the OC-OTEC flow diagram [42]: (1) warm seawater injected into the vacuum chamber flash evaporator; (2) flash evaporation of the warm seawater in a vacuum chamber; (3) expansion of the desalinated water vapor through a steam turbine generator; (4) return of most of the warm seawater from the evaporator to sea since only about 0.5% of the mass of the warm seawater entering the evaporator is converted into steam; (5) exit of desalinated low-pressure water vapor from the steam turbine; (6) condensation of the water vapor leaving the turbine (occurs by heat transfer to the cold seawater); (7) cold seawater return to sea, where since the evaporator produces desalinated steam, the condenser can be designed to produce desalinated water represented by (7^1) in Fig. 16; and (8) compression of the noncondensable gases to pressures required to discharge them from the system, e.g., gases that come out of the seawater solution under low operating pressure, such as oxygen, nitrogen, and carbon dioxide (essentially air). Note that the noncondensable gases are not released into the atmosphere but rather reinjected into the return water [42].

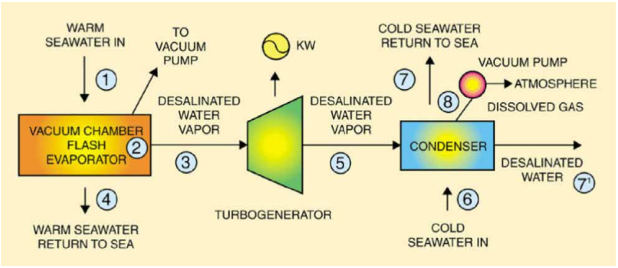

Fig. 16. *Open-cycle OTEC flow diagram. (Image courtesy of [1].)*

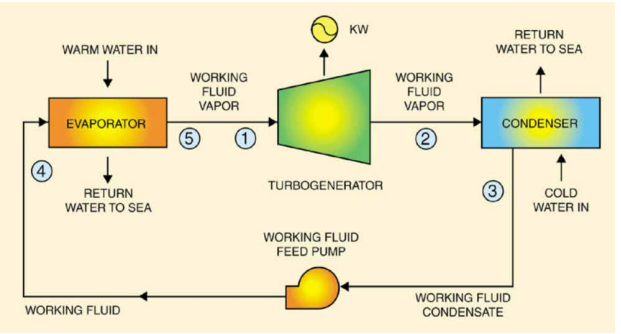

Fig. 17. *Closed-cycle OTEC process flow diagram. (Image courtesy of [41].)*

In order to generate a practical amount of electrical power in an OC-OTEC system, a large turbine is required to accommodate the relatively large volumetric flow rates of the low-pressure steam. Although the last stages of turbines used in conventional steam power plants can be adapted, existing technology limits the power that can be generated by a single turbine module to about 2.5 MW [42].

The first OC-OTEC plant was a land-based system built in 1930 in Cuba rated at 22 kW [42], [46]. While the plant operated for several weeks, it was not able to achieve net power production because of poor site selection, i.e., the thermal resource ΔT was not sufficient, as well as a power plant/seawater components design mismatch [42]. The only other open-cycle demonstration was a land-based 210-kW OC-OTEC Experimental Apparatus built and operated at the Natural Energy Laboratory of Hawaii Authority (NELHA) [42]. The system operated for six years (1993–1998), and provided data and analyses for future modifications and improvements in the OC-OTEC process. The turbine generator was designed for an output of 210 kW for 26 °C warm surface water and a deep water temperature of 6 °C. A fraction (10%) of the steam produced was diverted to a surface condenser for the production of desalinated water. The highest production rates achieved were 255 kW (gross) with a corresponding net power of 103 kW (due to auxiliary power required for the pumps and losses) and 0.4 L/s of desalinated water [42]. It must be noted that the net power was not optimized because pumping losses were relatively high due to the use of a seawater system that was already available. It is expected that for a commercial size plant the ratio of net to gross power would be about 0.7 [53].

D. Closed-Cycle OTEC

In closed-cycle OTEC (CC-OTEC) warm surface seawater provides heat to a working fluid with a low boiling point temperature to vaporize the working fluid to drive a turbine generator. Fig. 17 shows a simple flow diagram for CC-OTEC systems with steps including: (1) working fluid from an evaporator, warmed by surface seawater to produce working fluid vapor to drive a turbine generator; (2) working fluid vapor is then condensed by the cold water from the deep ocean; (3) working fluid in liquid form is then pumped back to the initial evaporator; (4) evaporator process is continued; and (5) completion of closed system with production of working fluid vapor. The commonly used working fluid is ammonia, although ammonia–water mixtures can also be used to vaporize and condense at the temperatures of the available seawater streams [42], [47].

Hybrid systems can combine both the open and closed cycles to maximize the use of the pumped seawater thermal resource available to produce both power and water [41]. For example, the steam generated by flash evaporation in OC-OTEC can then be used as the heat to drive a CC-OTEC process [54]. In addition, power can first be generated in a CC-OTEC system, and then the warm seawater can be flash evaporated in an OC-OTEC system, producing freshwater in the process [41], [43]. In addition, multiple-stage systems can use the warm and cold seawater more than once in multiple heat exchangers to increase power and freshwater production [42], [47].

In [42], a 10-MW CC-OTEC pilot plant is proposed based on state-of-the-art manufacturing and practices to represent a complete scaled version of a floating commercial size OTEC plant of 50 MW or larger. Optimized plant flow rates of 27.7 m^3/s of 4.5 °C cold water pumped from a depth of 1000 m, and 52.8 m^3/s of 26 °C warm water pumped from a depth of about 20 m, would yield a gross generator output power of 16 MW. The auxiliary power required for the pumps is 5.3 MW resulting in a net power output of 10.7 MW (~70% of the gross power output). To keep the pumping losses at ~30% of the gross power output, an average speed of less than 2 m/s is designed for the seawater flowing through the pipes transporting the seawater resource to the OTEC power plant. The floating plants could be located a few kilometers from land, transmitting the power to shore via submarine power cables, and could also include OC-OTEC plants and transport desalinated water to shore via flexible pipes [42].

E. OTEC Generator Grid Interface

OTEC generators would provide baseload power, where the steam turbines drive synchronous generators that have

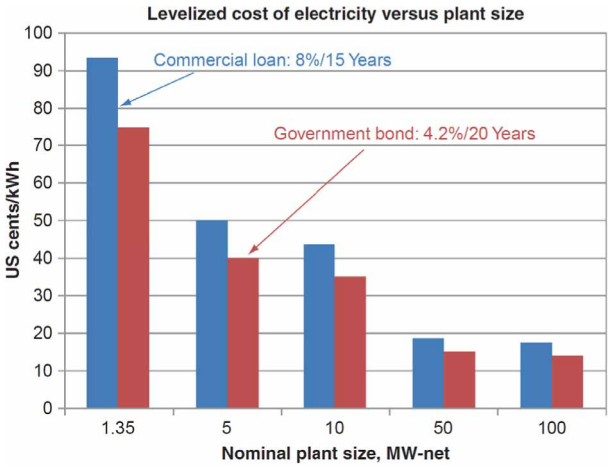

Fig. 18. *Cost of electricity (capital cost amortization + OMR&R levelized cost) production for first-generation OTEC plants as a function of plant size with loan terms (interest and term) as a parameter, and annual inflation is assumed constant at 3%. (Image courtesy of [42].)*

similar protection and grid interface as conventional thermal plants such as coal and natural gas. Generator grid interface is through stepup transformers, and again for floating plants, the power would be transmitted to shore via submarine power cables. Synchronizing equipment is employed to control the generator terminal voltages for grid voltage matching through the stepup transformers, as well as to control the turbine speed for grid frequency and phase regulation [42]. During plant startups, the generator voltage, frequency and phase are synchronized to the grid, the circuit breaker is energized and the OTEC generators are interfaced to the grid.

F. Cost

The estimated capital costs for OTEC plants are strongly related to the plant size and range from $7900/kW for a plant size of 100 MW, to more than $22 000/kW for plants of 5 MW or less [55]. Considering the operations, maintenance, repairs, and replacement (OMR&R) costs, and the fact that no fuel is purchased, Fig. 18 presents the levelized cost of energy (LCOE) analyses for first generation OTEC plants in cents per kilowatt hour as a function of plant size and loan terms [42]. At commercial scale, developers expect a rapid decrease in LCOE through experience and plant upscaling, leading to a LCOE of about 10–18 cents/kWh [46]. In addition, in many favorable sites in the tropics, potable water is a highly desired commodity that can be marketed to offset the price of OTEC-generated electricity [42].

IV. TIDAL AND OCEAN CURRENTS

Marine renewable energy can be harnessed from both tidal and nontidal ocean currents. Tidal current is the periodic ebb and flow of coastal tidal waters accompanying the rise and fall of the tides driven by the gravitational forces of the moon and sun, combined with the centrifugal force produced by the rotation of the Earth [56]. The gravitational force of the moon is 2.2 times larger than the gravitational force of the sun due to the moon being much closer to the Earth, which more than compensates for the higher mass of the sun [56]. Nontidal ocean currents include the more continuous currents in the general circulatory system of the oceans, which are intensified along western boundaries [57]. Many commonalities exist between the technologies designed to harness tidal currents and ocean currents, and thus they will be discussed together.

For tidal energy, there are two main approaches to energy conversion associated with the potential and kinetic energy components [56]. The first, more traditional approach, seeks to capture the potential energy created by the difference in sea level between high and low tides, i.e., the tidal range, using a tidal barrage, dam, or barrier to establish a head of water to power a turbine, similar to a hydroelectric dam [58]. More recent developments in tidal energy have focused on the kinetic energy of the tidal currents to drive turbines, similar to how wind turbines extract energy from the wind [59], [60]. Similar approaches are suitable for harnessing the kinetic energy in ocean currents. Many current turbine designs, also called tidal stream or marine current, resemble submerged wind turbines (see Fig. 19), though with a diversity of designs reminiscent of the early days of wind energy.

Most coastal sites experience high and low tides twice a day (semidiurnal tides), although some areas have just one high and low tide per day (diurnal tides) or a combination of diurnal and semidiurnal oscillations (mixed tides) [57]. Thus, tidal currents are variable in speed and reverse direction, however, they are uninfluenced by weather such that the variability is deterministic, not stochastic like wind or wave [59]. Despite the relatively low velocity of tidal currents, the higher density of water (832 times more dense than air) means that tidal turbines have the opportunity to extract more power for a given turbine rotor swept area than wind, and, thus, tidal turbines are generally smaller than wind for equivalent power capacities [61], [62]. While tides

Fig. 19. *Array of horizontal axis ANDRITZ HYDRO Hammerfest HS1000 tidal current turbines [66].*

can be accurately predicted years in advance, tidal generation is nondispatchable with typical capacity factors ranging from 10% to 40% [63]–[65].

Ocean currents are driven by wind patterns and the ocean thermohaline circulation caused by density gradients due to temperature and salinity differences [57]. Compared to tidal currents, ocean currents are unidirectional, and generally slower but more continuous than tidal currents, and while often located at deep ocean sites, they tend to be stronger near the surface [67]. Unlike tidal currents, ocean currents are influenced by atmospheric and ocean conditions and can experience "meandering" on scales of tens of kilometers [67].

A. Resource Characteristics

The worldwide tidal energy resource is on the order of 1000 GW and relatively localized [60]. Fig. 20 [68] illustrates the global amplitude of the main lunar tidal forcing and the white lines are lines of constant tidal phase, called cotidal lines, differing by 1 h. Along the cotidal lines the high tide is reached simultaneously, extending from the coast out into the ocean and converging at amphidromic points with minimal tide. The curved arcs around the amphidromic points show the direction of the tides, each indicating a synchronized 6-h period [68]. Fig. 20 indicates the potential for both barrage/range systems and tidal stream technologies, as high tidal ranges are often a prerequisite for fast tidal currents. Currents are often further magnified by topographical features, such as headlands, inlets and straits, or by the shape of the seabed when water is forced through narrow channels [69]. Generally, tidal streams must reach flow speeds of at least 1–2 m/s for tidal current turbines to operate cost effectively [57], [70]. Tidal currents exceeding 4 m/s can pose a significant design challenge due to the imparted load, while sites with peak velocities lower than 1 m/s are often considered uneconomical [71]. Major tidal streams have been identified along the coastlines of every continent, making it a global, though site specific, resource [57]. Total tidal barrage/range

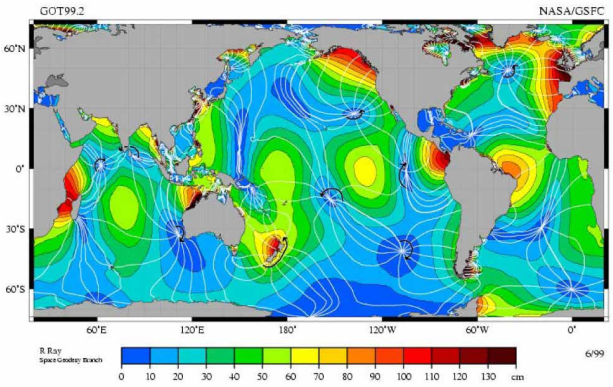

Fig. 20. ***Global distribution of semidiurnal tidal amplitude [68].***

deployment in 2015 was about 518 MW, and about 7 MW for tidal current. Extensive plans exist for tidal barrage projects in India, Korea, the Philippines, and Russia adding up to about 115 GW. Deployment projections for tidal current up to 2020 are in the range of 200 MW [60].

In the United States, the tidal and ocean current theoretical power potential is estimated at about 50 GW from tidal streams [72] and about 5 GW from the Gulf Stream Florida Current [73]. The U.S. tidal current resource hotspots are defined as current speeds of at least 1 m/s, total surface area larger than 0.5 km^2 and depths greater than 5 m [74]. The majority of the U.S. tidal current resource is found in Alaska, followed by Maine, Washington, Oregon, California, Massachusetts, and New York [74]. Note that tidal current technologies are scalable and suitable for deployment in river environments, and in the United States, the feasible average resource is estimated at 14 GW from rivers [75].

B. Tidal Barrage, Tidal Current, and Ocean Current Technologies

Tidal and ocean current technologies can be categorized into three main types: tidal barrage/range, tidal current turbines, and ocean current turbines. Tidal barrage is considered a mature technology, however, implementation has been limited due to site availability, environmental effects, and high capital costs [57]. Tidal and ocean current technologies are still undergoing research and development and are at the precommercial demonstration stage [57].

C. Tidal Barrage

Tidal barrage, or tidal range, technologies harvest power from the potential energy of the height difference between high and low tides. A tidal barrage is typically a dam or other barrier built across a bay or estuary, creating a reservoir (basin) behind it, such that the flow of water is forced into a smaller area to create a tidal range in excess of 5 m [56]. Tidal barrages operate much like a hydroelectric dam in that the barrage produces a pressure head to drive turbines, though tidal currents flow in both directions with generators designed to respond to two directional water flows [56].

The world's first large-scale tidal barrage/range power plant, the 240-MW La Rance Tidal Power Station, became operational in 1966 in Brittany, France and is still in operation today. The 254-MW Sihwa Lake Tidal Power Station in South Korea became the world's largest (and newest) tidal barrage when it was opened in 2011. Only a few other much smaller sites have been developed around the world [76].

D. Tidal Current and Stream Technologies

It is anticipated that commercial tidal current/stream projects will operate in arrays of turbines as tidal farms, similar to commercial utility scale wind farms [59], [77]. Many

of the tidal energy converter concepts at the forefront of the industry have adopted a horizontal axis turbine, with several design permutations within the horizontal axis design type [59]. An overview of tidal stream projects conducted in [60] revealed that about 76% are horizontal axis turbines, about 12% are vertical axis turbines, with other designs making up the remaining 12%.

Horizontal axis turbines—an example of which is shown in Fig. 19—are the marine equivalent of wind turbines where rotation of the turbine is due to the lift forces of the moving water on the turbine blades mounted on a horizontal axis [59], [78]. Thus, the turbines are similar to designs used for traditional wind turbines, however, due to the higher density of water relative to air, the blades are significantly smaller than equivalent power rated wind turbines and, due to lower current velocities, turn more slowly [60], [78].

To date, several developers have deployed single unit tidal current demonstration devices [59]. The world's first array of tidal power turbines to deliver power to the grid was deployed by Nova Innovation in the Bluemull Sound between the islands of Unst and Yell in the north of Shetland, where the North Sea meets the Atlantic. The second in a set of three Nova Innovation M100 100-kW turbines (see Fig. 21) was deployed in August 2016, lining up alongside the first turbine, which was installed in the Bluemull Sound in March 2016. The first commercial deployment of tidal turbines, the MeyGen project, consisting of four devices, each rated at 1.4 MW, was scheduled for installation in the Pentland Firth in northern Scotland toward the end of 2016.

E. Ocean Currents

The approaches and principles behind tidal current technologies can be adapted to generate power from ocean currents [57]. Compared to tidal currents, ocean currents are unidirectional and generally slower but more continuous. Ocean current technologies are in an early developmental stage, and to date, no full-scale prototype has been tested or demonstrated [57]. Although there are technology developers working on concepts in the United States, Japan, Italy, and Spain, they are much fewer in number than those developing tidal stream turbine concepts [57]. In the United States, the Southeast National Marine Renewable Energy Center (SNMREC) at Florida Atlantic University, seeks to advance ocean current technologies, specifically for the Gulf Stream Florida Current. Primary impediments to deployment of ocean current turbines include water depth (>300 m), which increases the complexity of mooring and electrical power export [57].

F. Power Electronics and Grid Interface

Due to the variable nature of tidal and ocean current resources, power electronic converters are employed to enable wide ranging speed control of the turbine generators to optimize power performance [78], [80], [81]. Tidal currents exhibit more variability than ocean currents, and are currently one of the most rapidly growing technologies for generating electric energy [82], and therefore tidal stream turbine grid interface will be the focus of this section.

A pure semidiurnal tidal cycle lasts 12 h and 25 min, where both ebb and flood occur once per cycle, and thus the tidal current varies and runs approximately six hours in one direction and then reverses for another six hours in the opposite direction. There are also periods of time when there is little or no horizontal flow of water, i.e., slack water, which occurs between the flood and ebb currents [56]. Fig. 22 presents an example of varying tidal current velocity, v m/s, and the resulting variable power output P_{el}, for one month [62]. A maximum tidal current velocity v_{max} of 2.5 m/s is assumed, along with a nominal generator power rating of 1 MW at v_{max} [62]. As seen from Fig. 22, maximum power is available every 14 days.

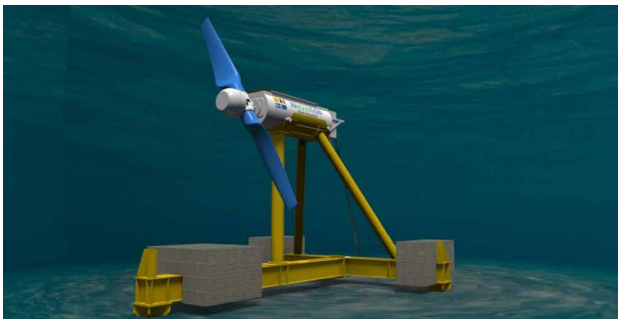

Fig. 21. *Nova Innovation M100 tidal current turbine [79].*

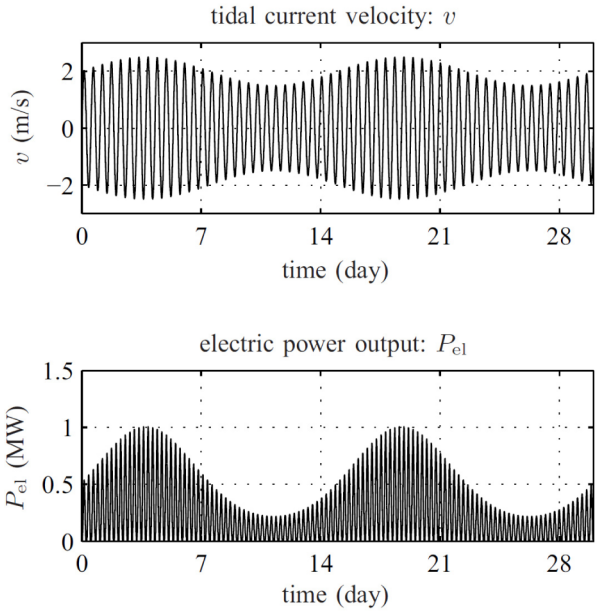

Fig. 22. *Tidal current velocity and power output for one month [62].*

The stream power that a tidal turbine extracts is proportional to the density of seawater and the cube of its speed, and can be expressed as follows:

$$P = \frac{1}{2}\rho C_p A v_{\text{tides}}^3 \tag{2}$$

where ρ (kg/m^3) is the seawater density, C_p is the power performance coefficient, A (m^2) is the cross-sectional area swept by the turbine blades, and v_{tides} (m/s) is the tidal stream velocity. The density of sea water ($\rho \approx 1025$ kg/m^3), at 832 times that of the air, enables tidal currents of about 1/9th the wind speed to carry comparable kinetic power density as wind [67]. The power performance coefficient (C_p) represents the percentage of the stream power that the turbine can extract, and is limited to ~ 59% by the well-known Betz law for sparse arrays. For tidal turbines, C_p (a function of tip speed ratio and blade pitch angle) [83] is generally in the range of 30%–50%, depending on the degrees of freedom for control in time-varying currents [82], [84]. Overall, (2) illustrates that the extracted power depends primarily on the tidal velocities and the turbine sizes.

As with the wave energy industry, commercial tidal stream projects are developing to operate in arrays of turbines, similar to utility scale wind farms [57], with submarine power cables connecting the devices/arrays to the grid through power electronic converters and stepup transformers. As such, tidal turbines can have a converter in each device, enabling every generator to operate at its optimum speed, or there can be a common converter for each array cluster, offshore or onshore [85]. In the case of one converter per array/cluster, the speed and electrical frequency vary proportionally with the average tidal current speed in the array/cluster. With only one converter per array/cluster, the resulting mechanical loads on the tidal current turbine drive trains could be higher than those tidal turbine systems with individual converters [64], where individual turbine converters will be discussed in more detail below.

Two commonly proposed tidal stream turbine converter technologies are [81], [82], [86]: 1) a doubly-fed induction generator (DFIG) configuration [87], [88], as shown in Fig. 23 [80]; and 2) a direct-drive permanent magnet synchronous generator (PMSG) [86], as shown in Fig. 24 [80]. Control approaches considered for tidal turbine converters are similar to those for DFIG and direct-drive PMSG for offshore wind turbines. Some control approaches use the generator side converter controller to maintain the rotational speed of the generator at an optimal value, and minimize core losses, while using the grid side converter controller to maintain the voltage of the dc link and to control the output reactive power. Other control approaches use the generator side converter controller to control the output active power and reactive power, while using the grid side converter controller for controlling the dc link voltage and the terminal voltage of the turbine system [82], [86]. As shown in Figs. 23 and 24, pitch controllers adjust the tidal current turbine to achieve optimum speeds [80]–[82].

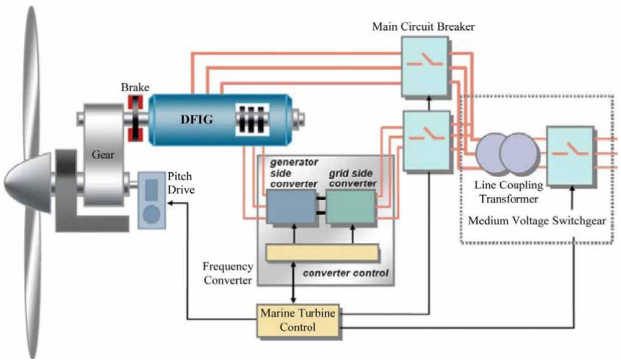

Fig. 23. *Schematic diagram of a DFIG-based generation system [80].*

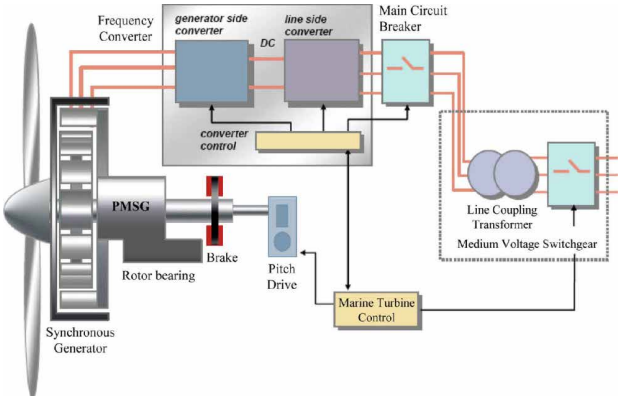

Fig. 24. *Schematic diagram of a PMSG-based generation system [80].*

G. Cost

There are a number of technological aspects that determine the performance and costs of tidal and ocean current technologies including: 1) conversion technology; 2) support structures; 3) array formation; and 4) electrical connections to shore [60].

The estimated capital costs for tidal barrage/range power generation is very site specific and is largely based on two large plants in operation, the La Rance barrage in France and the Sihwa dam in South Korea. Thus, the estimated capital costs range from $117/kW for the Sihwa, using an existing dam for the construction of the power generation technology, to about $340/kW for the La Rance barrage which was built for the purposes of power generation [60]. Electricity production costs for the La Rance and Sihwa installations are 5 cents/kWh and 2.5 cents/kWh, respectively [60].

Tidal current technologies are still largely in the demonstration stage, thus, capital cost estimates are projected to decrease as the level of deployment increases to large scale arrays as the industry enters a post-commercialization phase [46], [60]. Significant cost reduction is anticipated in the areas of installation, grid connection, and project

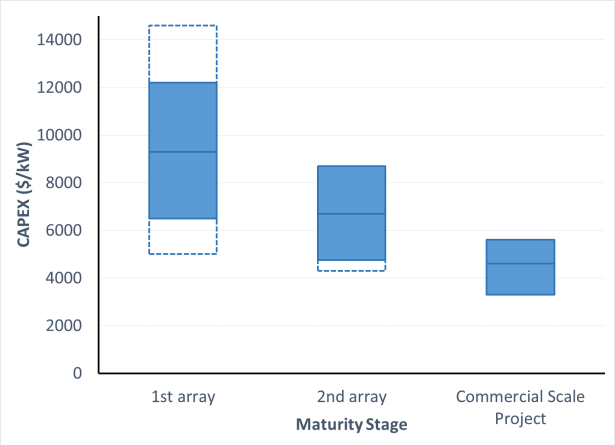

Fig. 25. ***Capital cost ranges for differing stages of deployment. (Adapted from [46].)***

development. Fig. 25 gives capital cost ranges for differing stages of deployment [46]. The dotted lines in Fig. 25 represent the max/min cost values provided from stakeholder engagements. The solid lines with shaded areas represent the industry averaged cost with an uncertainty bound of ±30%, with the exception of when the max or min from consultation falls below the ±30% uncertainty limit [46].

Fig. 26 gives levelized cost of energy (LCOE) ranges for differing stages of deployment, which are diverse within the first array deployment, and converge as progression is made toward commercial scale projects [46]. Again, the dotted lines in Fig. 26 represent the max/min costs provided from stakeholder engagements. The solid lines with shaded areas represent the industry-averaged cost with an uncertainty bound of ±30% [46]. Given the stage of development, these forecasts should be considered to have significant uncertainty, which will decrease over time as larger arrays enter service and reliability becomes more established.

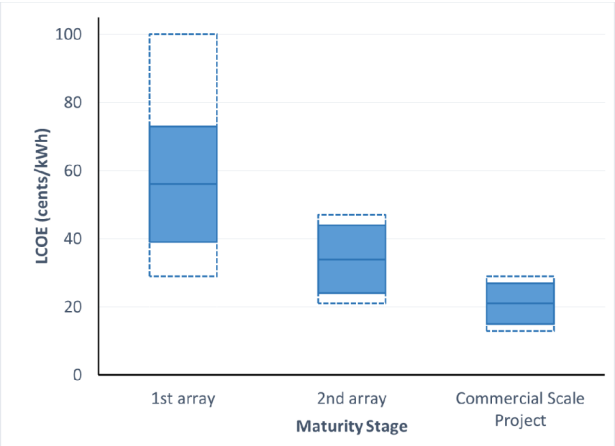

Fig. 26. ***The LCOE ranges at differing stages of deployment. (Adapted from [46].)***

V. GEOTHERMAL ENERGY SYSTEMS

Geothermal energy is an abundant, renewable (i.e., naturally replenished) resource consisting of the natural heat generated and stored in rock and fluids in the Earth's crust that can be used for electricity generation and for heating and cooling purposes. The heat is the resource, where steam or liquids, such as water or brine, from as deep as 6 mi (10 km) beneath the Earth's surface [89], serve as the medium that can be tapped to generate electricity through geothermal power plants operating steam turbine generators (see Fig. 27). Geothermal energy has significant advantages as a baseload renewable resource in that it is dispatchable and can provide around-the-clock generation and balancing of diurnal and weather-driven variable renewables such as solar and wind. Capacity factors of geothermal power plants can reach up to 95% [57]. In addition to electricity production, lower temperature geothermal at shallow depths, i.e., 10 °C–15 °C at 10 ft (3 m) below ground level, drives geothermal heat pumps (GHPs) for energy-efficient heating and cooling, and to provide hot water. GHPs use the relatively constant temperature of the Earth as a heat source in the winter and as a heat sink in summer. In the winter, GHPs use conventional vapor compression (refrigerant-based) heat pumps to extract the heat from the relatively warmer Earth to provide building heat. In the summer, the process reverses and the GHP pulls the building's warmer air into the relatively cooler ground, where the excess energy in these processes can be used to heat water [90]. The remainder of this geothermal section will focus on power generation.

A naturally occurring geothermal system is defined by three key elements: heat, fluid, and permeability at depth. In order to access heat, fluid must come into contact with heated rock, either via natural fractures or through stimulating the rock [91]. High temperatures are continuously produced inside the Earth, primarily due to the slow decay of radioactive particles in the rock [1]. Geothermal resources

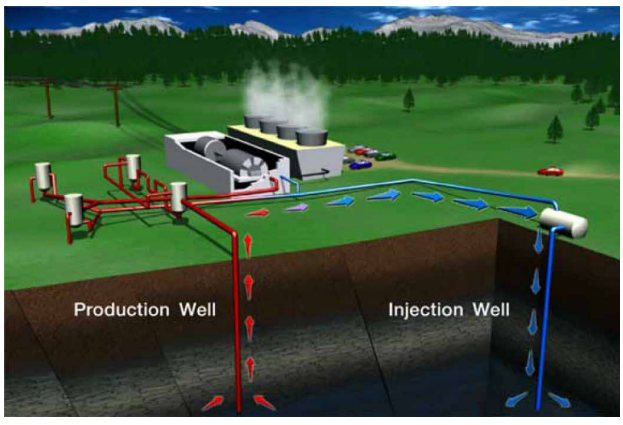

Fig. 27. ***Natural steam from production wells power steam turbine generators. The steam is condensed by evaporation in the cooling tower and pumped down injection wells to sustain production. (Image courtesy of the Geothermal Energy Association.)***

can be classified as low temperature (less than 90 °C), moderate temperature (90 °C–150 °C), and high temperature (greater than 150 °C). Surrounding the Earth's core of solid iron, about 4000 mi (~6500 km) below the Earth's surface, is an outer core of very hot magma (melted rock). Surrounding the outer core is the mantle, which is about 1800 mi thick and made of magma and rock. The outermost layer of the Earth is the crust, ranging from 3–35 mi (4.8–56 km) thick, about 3–5 mi thick under the oceans and 15–35 mi thick on the continents [1]. The crust is divided into pieces called plates which drift apart and push against each other in a process called plate tectonics. Magma comes close to the Earth's surface near the edges of these plates, which is also the location of volcanic and seismic activity. Most high-temperature geothermal resources (150 °C–370 °C) occur where magma has penetrated the upper crust of the Earth around these tectonic plate boundaries where the crust is highly fractured and thus permeable to fluids. The magma heats the surrounding rock, and when the rock is permeable enough to allow the circulation of water, the resulting hot water or steam is referred to as a hydrothermal resource for geothermal power plants [90].

Geothermal energy production has historically been concentrated in areas where the geological conditions permit naturally occurring steam or hot water reservoirs to transfer heat from within the Earth to the surface [92]. In contrast to conventional geothermal systems, enhanced geothermal systems (EGS), also known as engineered geothermal systems, target geothermal locations with insufficient natural permeability or fluid saturation, i.e., regions of hot dry and impermeable rock. EGS technologies enhance and/or create geothermal resources in what is called hot dry rock (HDR) through hydraulic stimulation. To develop an EGS, pressurized fluid (typically water) is injected into the subsurface where the increased fluid pressure coupled with thermal stresses, due to the temperature difference between the hot rock and cooler water, create new fractures and open existing fractures in the rock fabric to enhance the permeability [93]. Thus, the EGS concept is to create large heat exchange areas in hot fractured rock to which water can be added through injection wells. The injected water absorbs heat and generates steam by contact with the rock and returns to the surface through production wells to a geothermal power plant. Geothermal injection and production wells are constructed of pipes layered inside one another and cemented into the Earth and to each other, protecting shallow drinking water aquifers from mixing with deeper geothermal water/brine. It is estimated that 90% of the geothermal power resource in the United States exists through EGS [94].

A. Resource Characteristics

The global geothermal market is at about 13.3 GW of operating capacity as of 2016, spread across 24 countries, where the global geothermal industry is expected to reach approximately 18.4 GW by 2021. It is estimated that there is over 200 GW of conventional hydrothermal potential globally available based on current knowledge and technology [95]. Fig. 28 depicts global operating capacity by country.

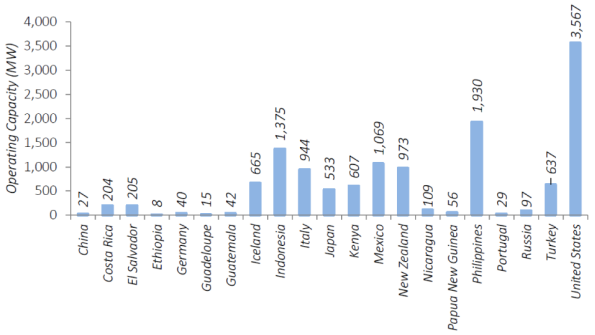

Fig. 28. ***Geothermal power operating capacity by country [95].***

Fig. 29 provides the current planned capacity additions under development. With these planned capacity additions, only about one sixth of the global potential has identifiable development plans [95].

The geothermal resource potential map in Fig. 30 shows the U.S. locations of identified hydrothermal sites and favorability of deep EGS.

B. Geothermal Power Plant Technologies

Three primary types of geothermal power plant designs make use of the various temperature ranges of geothermal resources: dry steam, flash steam, and binary cycle. Binary plants are used with lower temperature resources while flash and dry steam plants are used with higher temperature resources. Flash technologies, including double and triple flash, account for almost two-thirds of installed capacity globally, while dry steam makes up about a quarter, and binary makes up about a sixth of global geothermal power generation [95]. The overall energy conversion efficiency, based on the total heat content (enthalpy) of the produced geothermal resource/fluid, is affected by many parameters

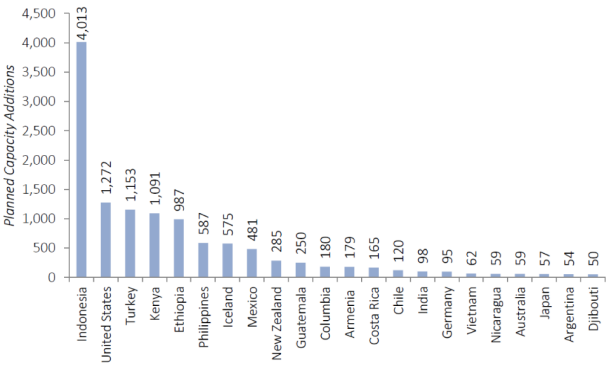

Fig. 29. ***MW capacity under development by country [95].***

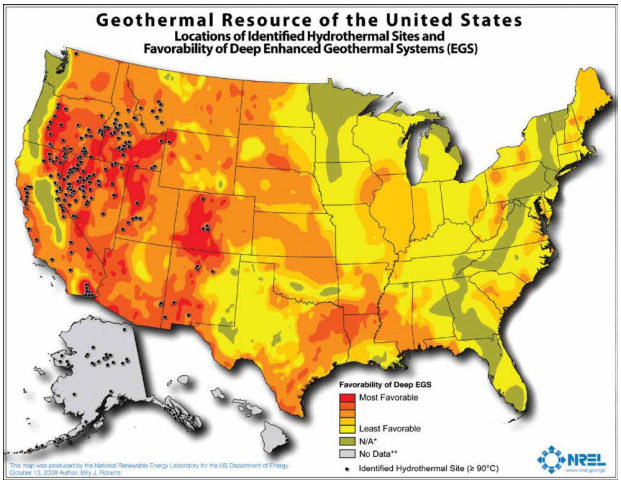

Fig. 30. ***Geothermal resource potential map for the United States. "Hydrothermal" refers to naturally occurring geothermal resources used by conventional geothermal power plants, while "Deep EGS" refers to geothermal heat resources that require technologies that are currently being developed and demonstrated. (Image courtesy of NREL.)***

including the power plant design (dry steam, single, double or triple flash, binary, or hybrid system), size, the geothermal resource temperature as well as ambient surface temperatures. The conversion efficiencies of geothermal power plants are generally lower than that of conventional thermal plants (such as coal and natural gas), and range from 11% to 22% for geothermal resource/fluid temperatures ranging from 150 °C to 350 °C, respectively [89].

C. Dry Steam

Dry steam power plants (Fig. 31) draw from underground reservoirs producing mostly steam that is heated by the mantle and released through natural vents. Production

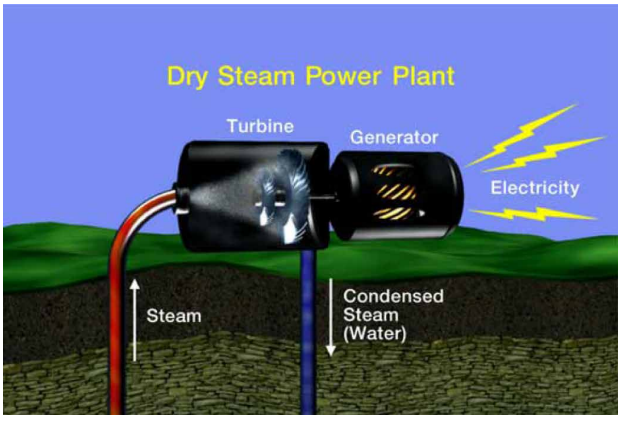

Fig. 31. ***Geothermal dry steam power plant, where the steam shoots up the wells and is passed through a rock catcher (not shown) and then directly into the turbine. (Image courtesy of the Geothermal Energy Association.)***

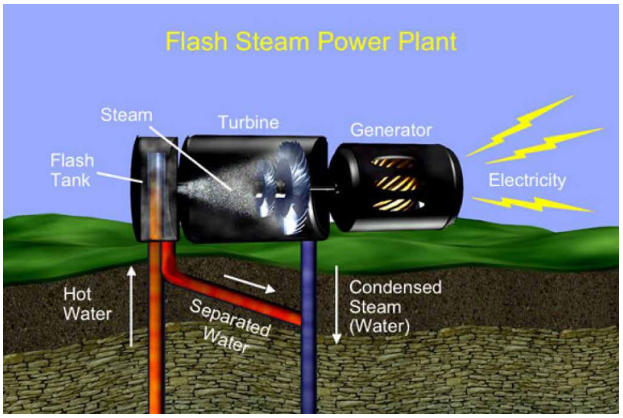

Fig. 32. ***Flash steam power plants use hot water reservoirs. As the hot water is released from the pressure of the deep reservoir in a flash tank, some if it flashes to steam. (Image courtesy of the Geothermal Energy Association.)***

wells are drilled down to the aquifer and the superheated, pressurized steam (180 °C–350 °C) is brought to the surface through pipelines, filtered/purified (e.g., through a "rock-catcher" to protect the turbine) and passed/expanded through a steam turbine. The lower pressure steam is then cooled and condensed into water using water from a cooling tower. The steam turbine is directly coupled to the generator, and the condensate is pumped back to the cooling tower where it is cooled and then recirculated to the condenser located at the exit of the steam turbine. Excess condensate, as well as external water pumped in to replenish the resource (e.g., from wastewater plants) is injected back into the reservoir through injection wells [95], [96].

D. Flash Steam

Flash geothermal power plants, depicted in Fig. 32, are the most common (about two-thirds of installed capacity), and use water-dominated geothermal reservoirs with temperatures greater than 182 °C. The boiling point of a fluid increases as its pressure is increased, and thus superheated water in geothermal reservoirs is liquid water under pressure at a temperature higher than the normal boiling point of 100 °C. When the pressure is reduced the water flashes to steam. Thus, as the superheated water is pumped from depth, the pressure decreases and some of the hot water boils, or "flashes" into steam in a separator, or flash tank. The separated and purified steam is piped to a steam turbine/generator and the remaining hot water may be flashed again (twice, i.e., double flash plant) or three times (triple flash) at progressively lower pressures and temperatures, to obtain more steam [92]. The cooled brine and the condensate are typically sent back down into the reservoir through injection wells. Combined-cycle flash steam plants use the heat from the separated geothermal brine in lower temperature binary plants (discussed next) to produce additional power before reinjection [92].

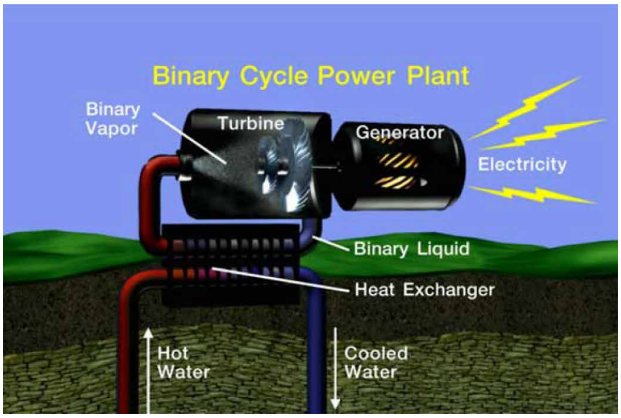

Fig. 33. *Binary power plant, where the heat from geothermal water is used to vaporize a working fluid in separate adjacent pipes. The vapor, like steam, powers the turbine generator. (Image courtesy of the Geothermal Energy Association.)*

E. Binary Cycle

For geothermal temperatures less than 182 °C, binary cycle power plants (see Fig. 33) are employed where the hot water or brine emerging from depth through a borehole is directed through a heat exchanger to boil a working fluid, typically an organic compound with a lower boiling point than water (e.g., butane or pentane in the organic Rankine cycle and an ammonia–water mixture in the Kalina cycle) [92]. The working fluid vaporized in the heat exchanger is used to drive a steam turbine, where the water/brine from depth is then recycled back down the injection borehole to be reheated. The water and the working fluid are kept separate during the entire process, so there are little or no air emissions, and the water/brine from the primary heat source never comes in contact with the turbine generator units.

F. Geothermal Generator Grid Interface

Geothermal energy systems provide baseload power, where the steam turbines drive synchronous generators that have similar protection and grid interface as conventional thermal plants such as coal and natural gas. The external generator excitation system provides variable dc to the field winding for controlling terminal voltages and reactive power, ensuring stable operation with the grid, improving transient stability after faults, and keeping the machinery within acceptable operating ranges [97]. The steam governor system controls the position of the steam governing valve to regulate turbine speed, power, and frequency synchronization to the grid. Generator grid interface is through stepup transformers. Synchronizing equipment is employed to control the generator terminal voltages for grid voltage matching through the stepup transformers, as well as to control the turbine speed for grid frequency and phase regulation. When the generator voltage, frequency and phase are synchronized to the grid, the circuit breaker is energized and the geothermal generator is interfaced to the grid [97].

Table 1 Large-Scale Development Cost and TRL Estimates

Technology	Cost of energy (cents/kWh)	Capacity cost ($/W)	TRL
Wave	10 to 15	3 to 5	7-8
OTEC	10 to 18	8 to 22	6
Tidal (barrage)	2.5 to 5	0.12 to 0.34	9
Tidal (stream) and ocean currents	10 to 25	3 to 5	8
Geothermal	3 to 15	3 to 6.5	9

G. Cost

The capital costs for a geothermal plant range from $3000 to more than $6500/kW, and are highly dependent on the type and temperature of the hydrothermal resource, the conversion technology, and the necessary depth of the wells [98]. Geothermal plants harnessing high-temperature resources (flash and dry steam systems) tend to be less expensive than those relying on low-temperature resources (binary systems). Considering the operating and maintenance costs, and the fact that no fuel is purchased, levelized cost analyses reveal that geothermal plants can produce electricity for 3–15 cents/kWh, depending on the resource characteristics and the project development finance structure [98]–[100].

VI. CONCLUSION

This paper presents techno–economic summaries of ocean wave, tidal, marine current, ocean thermal, and geothermal energy, in addition to the aspects of grid interface. The total global average wave resource is estimated at approximately 2000 GW [7], with approximately 300 GW in the United States [5]. The total global tidal resource is estimated at approximately 1000 GW, with 50 GW in the United States [60], [72]. The marine current resource estimate for the Florida Current in the southeast United States is estimated at 5 GW [73]. Ocean thermal has a global capacity estimate of 5000 GW [48]. Last, the global geothermal capacity estimate is approximately 200 GW, but with much more possible through enhanced geothermal systems [95].

Cost information can be presented as both near-term early-industry projects and prototypes and projected large-scale development future costs.

For near-term cost, it was found that wave energy conversion has a median of $0.24/kWh for 16 studies [25] (long term projected to $0.10-$0.15/kWh). Tidal is found to be approximately $0.50/kWh and $0.20/kWh depending on stage of development [46] (long term projected to $0.025-$0.25/kWh, depending on type). Ocean thermal long-term cost is projected to $0.10–$0.18/kWh [46]. And

last, geothermal—being more closely aligned in technology with traditional coal, natural gas, and nuclear—is estimated at \$0.03–\$0.15/kWh [98]–[100].

A summary of the estimated long-term large-scale future cost of energy and capacity is given in Table 1. The table also includes an estimate of the Technology Readiness Level (as defined by the U.S. Department of Energy).

Costs for transmission and grid connection are not included in the estimates, but should be considered. On shore systems can work with standard ac power transmission and protection equipment. Offshore systems require transmission of the power to shore, which can be implemented as ac or dc transmission (with dc to ac conversion at the shore point of connection to the bulk grid) [101]–[104]. The cost of high-power undersea transmission cables is approximately on the order of \$3.3 million per mile (\$2 million per kilometer) [105].

Considering the raw potential of these resources, along with costs commensurate with early stage technologies, it is indicated that continued development may reveal these resources to be important components of a diverse energy mix. ■

Acknowledgment

The authors gratefully acknowledge the help of L. Vega of the Hawaii National Marine Renewable Energy Center; B. Polagye of the University of Washington; and K. Gawell of the Geothermal Energy Association.

REFERENCES

[1] S. M. R. Tousif and S. M. B. Taslim, "Producing electricity from geothermal energy," in *Proc. IEEE Environ. Elect. Eng. Int. Conf. (EEEIC)*, May 2011, pp. 1–4.

[2] D. A. Halamay, T. K. A. Brekken, A. Simmons, and S. McArthur, "Reserve requirement impacts of large-scale integration of wind, solar, and ocean wave power generation," *IEEE Trans. Sustain. Energy*, vol. 2, no. 3, pp. 321–328, Jul. 2011.

[3] G. García-Medina, H. T. Özkan-Haller, and P. Ruggiero, "Wave resource assessment in Oregon and southwest Washington, USA," *Renew. Energy*, vol. 64, pp. 203–214, Apr. 2014.

[4] R. Shaw, *Wave Energy: A Design Challenge*. Ellis Horwood Ltd., 1982.

[5] *Mapping and Assessment of the United States Ocean Wave Energy Resource*, Electric Power Research Institute, Palo Alto, CA, USA, 2011, p. 1024637.

[6] *Annual Energy Outlook 2016 with Projections to 2040*, Energy Information Administration, Washington, DC, USA, Aug. 2016.

[7] K. Gunn and C. Stock-Williams, "Quantifying the global wave power resource," in *Proc. 4th Int. Conf. Ocean Eng.*, 2012.

[8] A. Babarit *et al.*, "Numerical benchmarking study of a selection of wave energy converters," *Renew. Energy*, vol. 41, pp. 44–63, May 2012.

[9] T. K. A. Brekken, K. Rhinefrank, A. von Jouanne, A. Schacher, J. Prudell, and E. Hammagren, "Scaled development of a novel wave energy converter including numerical analysis and high-resolution tank testing," *Proc. IEEE*, vol. 101, no. 4, pp. 866–875, Apr. 2013.

[10] A. F. O. Falcão and J. C. C. Henriques, "Oscillating-water-column wave energy converters and air turbines: A review," *Renew. Energy*, vol. 85, pp. 1391–1424, Jan. 2016.

[11] N. Delmonte, D. Barater, F. Giuliani, P. Cova, and G. Buticchi, "Oscillating water column power conversion: A technology review," in *Proc. IEEE Energy Convers. Congr. Expo. (ECCE)*, Sep. 2014, pp. 1852–1859.

[12] J. Cruz, *Ocean Wave Energy: Current Status and Future Perspectives*. Springer, 2008.

[13] H. Polinder and M. Scuotto, "Wave energy converters and their impact on power systems," in *Proc. Int. Conf. Future Power Syst.*, 2005, pp. 1–9.

[14] R. So, S. Casey, S. Kanner, A. Simmons, and T. K. A. Brekken, "PTO-Sim: Development of a power take off modeling tool for ocean wave energy conversion," in *Proc. IEEE Power Energy Soc. General Meeting*, Jul. 2015, pp. 1–5.

[15] J. V. Ringwood, G. Bacelli, and F. Fusco, "Energy-maximizing control of wave-energy converters: The development of control system technology to optimize their operation," *IEEE Control Syst. Mag.*, vol. 34, no. 5, pp. 30–55, Oct. 2014.

[16] T. Brekken, B. Batten, and E. Amon, "From blue to green [ask the experts]," *IEEE Control Syst.*, vol. 31, no. 5, pp. 18–24, Oct. 2011.

[17] N. Müller, S. Kouro, M. Malinowski, S. Rivera, and B. Wu, "Cascaded H-bridge multilevel converter interface for Wave Dragon energy conversion system," in *Proc. IEEE Ind. Electron. Soc. (IECON)*, Nov. 2013, pp. 6201–6206.

[18] N. Müller, S. Kouro, J. Glaria, and M. Malinowski, "Medium-voltage power converter interface for Wave Dragon wave energy conversion system," in *Proc. IEEE Energy Convers. Congr. Expo. (ECCE)*, Sep. 2013, pp. 352–358.

[19] E. Amon, T. K. A. Brekken, and A. von Jouanne, "A power analysis and data acquisition system for ocean wave energy device testing," in *Proc. Appl. Power Electron. Conf. (APEC)*, 2009, pp. 750–754.

[20] P. Igic *et al.*, "Multi-megawatt offshore wave energy converters—Electrical system configuration and generator control strategy," *IET Renew. Power Generat.*, vol. 5, no. 1, pp. 10–17, Jan. 2011.

[21] M. P. Kazmierkowski and M. Jasinski, "Power electronic grid-interface for renewable ocean wave energy," in *Proc. Workshop Compat. Power Electron. (CPE)*, 2011, pp. 457–463.

[22] M. Jasinski, "Vector control of AC/DC/AC converter—Generator subset in wave-to-wire power train for wave dragon MW," in *Proc. EUROCON*, 2007, pp. 1324–1327.

[23] M. Jasinski *et al.*, "Control of AC/DC/AC converter for multi MW wave dragon offshore energy conversion system," in *Proc. IEEE Int. Symp. Ind. Electron.*, Jun. 2007, pp. 2685–2690.

[24] T. Ahmed, K. Nishida, and M. Nakaoka, "Grid power integration technologies for offshore ocean wave energy," in *Proc. IEEE Energy Convers. Congr. Expo. (ECCE)*, Sep. 2010, pp. 2378–2385.

[25] R. Alcorn and D. O'Sullivan, "Electrical design for ocean wave and tidal energy systems," *IET*, 2013.

[26] K. Rhinefrank *et al.*, "IEEE standards for oscillating machines to advance direct-drive wave energy generators," in *Proc. IEEE Power Energy Soc. General Meeting*, Jul. 2015, pp. 1–5.

[27] T. K. A. Brekken, H. M. Hapke, C. Stillinger, and J. Prudell, "Machines and drives comparison for low-power renewable energy and oscillating applications," *IEEE Trans. Energy Convers.*, vol. 25, no. 4, pp. 1162–1170, Dec. 2010.

[28] M. P. Kazmierkowski and M. Jasinski, "Power electronics for renewable sea wave energy," in *Proc. 12th Int. Conf. Optim. Electr. Electron. Equip. (OPTIM)*, May 2010, pp. 4–9.

[29] M. Alberdi, M. Amundarain, A. Garrido, I. Garrido, and F. J. Maseda, "Fault-ride-through capability of oscillating-water-column-based wave-power-generation plants equipped with doubly fed induction generator and airflow control," *IEEE Trans. Ind. Electron.*, vol. 58, no. 5, pp. 1501–1517, May 2011.

[30] K. Biligiri, "Grid emulator for wave energy converter testing," M.S. thesis, Oregon State Univ., Corvallis, OR, USA, 2014.

[31] A. Blavette, D. O'Sullivan, R. Alcorn, T. Lewis, and M. Egan, "Impact of a medium-size wave farm on grids of different strength levels," *IEEE Trans. Power Syst.*, vol. 29, no. 2, pp. 917–923, Mar. 2014.

[32] D. B. Murray, J. G. Hayes, D. L. O'Sullivan, and M. G. Egan, "Supercapacitor testing for power smoothing in a variable speed offshore wave energy converter," *IEEE J. Ocean. Eng.*, vol. 37, no. 2, pp. 301–308, Apr. 2012.

[33] S. Muthukumar, S. Kakumanu, S. Sriram, and V. Jayashankar, "Energy storage considerations for a stand-alone wave energy plant," in *Proc. IEEE Int. Conf. Electr. Mach. Drives*, May 2005, pp. 193–198.

[34] T. K. A. Brekken, H. T. Ozkan-Haller, and A. Simmons, "A methodology for large-scale ocean wave power time-series generation," *IEEE J. Ocean. Eng.*, vol. 37, no. 2, pp. 294–300, Apr. 2012.

[35] M. Santos *et al.*, "Integrating wave and tidal current power: Case studies through modelling and simulation," in *Proc. Int. Energy Agency Implementing Agreement Ocean Energy Syst.*, 2011, p. T0331.

[36] J. Khan, D. Leon, A. Moshref, S. Arabi, and G. Bhuyan, "Network security assessments for integrating large-scale tidal current and ocean wave resources into future electrical grids," *Proc. IEEE*, vol. 101, no. 4, pp. 956–977, Apr. 2013.

[37] D. Halamay and T. K. A. Brekken, "Monte Carlo analysis of the impacts of high renewable power penetration," in *Proc. Energy Convers. Congr. Expo. (ECCE)*, 2011, pp. 3059–3066.

[38] S. C. Parkinson, K. Dragoon, G. Reikard, G. García-Medina, H. T. Özkan-Haller, and T. K. A. Brekken, "Integrating ocean wave energy at large-scales: A study of the US Pacific Northwest," *Renew. Energy*, vol. 76, pp. 551–559, Apr. 2015.

[39] A. F. de O. Falcão, "Wave energy utilization: A review of the technologies," *Renew. Sustain. Energy Rev.*, vol. 14, no. 3, pp. 899–918, 2010.

[40] J. Chozas, "International levelised cost of energy for ocean energy technologies," *Ocean Energy Syst.*, 2015.

[41] L. Vega, "Ocean thermal energy conversion primer," *Marine Technol. Soc. J.*, vol. 6, no. 4, pp. 25–35, Dec. 2002.

[42] L. Vega, "Ocean thermal energy conversion," in *Encyclopedia of Sustainability Science and Technology*. Springer, 2012, pp. 7296–7328.

[43] *Ocean Thermal Energy Conversion, Technology Brief 1*, International Renewable Energy Agency, Masdar, United Arab Emirates, 2014.

[44] A. Hossain, A. Azhim, A. B. Jaafar, M. N. Musa, S. A. Zaki, and D. N. Fazreen, "Ocean thermal energy conversion: The promise of a clean future," in *Proc. IEEE Conf. Clean Energy Technol. (CEAT)*, Nov. 2013, pp. 23–26.

[45] A. G. Neto, L. Hiron, F. M. Pimenta, and R. R. Rodrigues, "Northeast Brazil potential for land-based OTEC implementation," in *Proc. IEEE Conf. Ecol. Veh. Renew. Energies (EVER)*, Mar. 2014, pp. 1–4.

[46] *International Levelised Cost of Energy for Ocean Energy Technologies*, Ocean Energy Systems (OES) and International Energy Agency (IEA), 2015.

[47] "Ocean thermal extractable energy visualization," Lockheed Martin Mission Systems Sensors, Washington, DC, USA, Tech. Rep. DE-EE0002664, 2012.

[48] G. C. Nihous, "A preliminary assessment of ocean thermal energy conversion resources," *J. Energy Resour. Technol.*, vol. 129, no. 1, pp. 10–17, 2007.

[49] K. Rajagopalan and G. C. Nihous, "Estimates of global ocean thermal energy conversion (OTEC) resources using an ocean general circulation model," *Renew. Energy J.*, vol. 50, pp. 532–540, Feb. 2013.

[50] L. R. Berger and J. A. Berger, "Countermeasures to microbiofouling in simulated ocean thermal energy conversion head exchangers with surface and deep ocean waters in Hawaii," *J. Appl. Environ. Microbiol.*, vol. 51, pp. 1186–1198, Jun. 1986.

[51] G. C. Nihous, "Mapping available Ocean Thermal Energy Conversion resources around the main Hawaiian Islands with state-of-the-art tools," *J. Renew. Sustain. Energy*, vol. 2, no. 4, p. 043104, 2010.

[52] H. Aydin, H. Lee, H. Kim, S. K. Shin, and K. Park, "Off-design performance analysis of a closed-cycle ocean thermal energy conversion system with solar thermal preheating and superheating," *Renew. Energy J.*, vol. 72, pp. 154–163, Dec. 2014.

[53] L. Vega and D. Evans, "Operation of a small open-cycle OTEC experimental facility," in *Proc. Ocean Int.*, vol. 5. Jan. 1994.

[54] R. H. Charlier and J. R. Justus, *Ocean Energies: Environmental, Economic, and Technological Aspects of Alternative Power Sources*. 1993.

[55] L. A. Vega, "Economics of ocean thermal energy conversion (OTEC): An update," in *Proc. Offshore Technol. Conf.*, 2010.

[56] F. O. Rourke, F. Boyle, and A. Reynolds, "Tidal energy update 2009," *Appl. Energy*2, vol. 87, no. 2, pp. 398–409, 2010.

[57] *Ocean Energy Technology Readiness, Patents, Deployment Status and Outlook*, International Renewable Energy Agency, Masdar, United Arab Emirates, Aug. 2014.

[58] J. Xia, R. A. Falconer, B. Lin, and G. Tan, "Estimation of annual energy output from a tidal barrage using two different methods," *Elsevier J. Appl. Energy*, vol. 93, pp. 327–336, May 2012.

[59] *Ocean Energy: State of the Art*, Strategic Initiative Ocean Energy, 2012.

[60] *Tidal Energy, Technology Brief 3*, International Renewable Energy Agency, Abu Dhabi, United Arab Emirates, Jun. 2014.

[61] A. S. Bahaj, "Marine current energy conversion: The dawn of a new era in electricity production," *Philosophical Trans. Roy. Soc.*, Jan. 2013.

[62] M. Kuschke and K. Strunz, "Modeling of tidal energy conversion systems for smart grid operation," in *Proc. IEEE Power Energy Soc. General Meeting*, Jul. 2011, pp. 1–3.

[63] E. Denny, "The economics of tidal energy," *Energy Policy*, vol. 37, no. 5, pp. 1914–1924, 2009.

[64] M. Santos *et al.*, "Integrating wave and tidal current power: Case studies through modelling and simulation," *Int. Energy Agency*, 2011.

[65] K. Tsuji, K. Naoi, M. Shiono, and K. Suzuki, "Study on the gear ratio for a tidal current power generation system using the MPPT control method," *J. Ocean Wind Energy*, vol. 2, no. 2, pp. 113–120, May 2015.

[66] *Islay Energy Trust*. [Online]. Available: https://islayenergytrust.org.uk/tidal-energy-project

[67] X. Yang *et al.*, "National geodatabase of ocean current power resource in USA," *Renew. Sustain. Energy Rev.*, vol. 44, pp. 496–507, Apr. 2015.

[68] G. D. Egbert and R. D. Ray, "Estimates of M_2 tidal energy dissipation from TOPEX/Poseidon altimeter data," *J. Geophyiscal Res.*, vol. 106, no. 10, pp. 22475–22502, 2001.

[69] *European Marine Energy Center (EMEC)*. [Online]. Available: http://www.emec.org.uk

[70] M. Palodichuk, B. Polagye, and J. Thomson, "Resource mapping at tidal energy sites," *IEEE J. Ocean. Eng.*, vol. 38, no. 3, pp. 433–446, Jul. 2013.

[71] T. Aboul-Seoud and A. M. Sharaf, "Utilization of the modulated power filter compensator scheme for grid connected tidal energy utilization systems," in *Proc. IEEE Power Energy Soc. General Meeting*, Oct. 2009, pp. 1–6.

[72] "Assessment of energy production potential from tidal streams in the United States," Georgia Tech Research Corporation, Atlanta, GA, USA, Tech. Rep. DE-FG36-08GO18174, 2011.

[73] X. Yang, K. A. Haas, and H. M. Fritz, "Evaluating the potential for energy extraction from turbines in the gulf stream system," *Renew. Energy*, vol. 72, pp. 12–21, Dec. 2014.

[74] Z. Defne *et al.*, "National geodatabase of tidal stream power resource in USA," *Renew. Sustain. Energy Rev.*, vol. 16, no. 5, pp. 3326–3338, 2012.

[75] *Assessment and Mapping of the Riverine Hydrokinetic Energy Resource in the Continental United States*, Electrical Power Research Institute, 2012.

[76] "Ocean energy systems," Tech. Rep., 2015.

[77] J. Khan, D. Leon, A. Moshref, S. Arabi, and G. Bhuyan, "Network security assessments for integrating large-scale tidal current and ocean wave resources into future electrical gridsids," *Proc. IEEE*, vol. 101, no. 4, pp. 956–977, Apr. 2013.

[78] D. O'Sullivan, D. Mollaghan, A. Blavette, and R. Alcorn, "Dynamic characteristics of wave and tidal energy development of a generic model for grid connection," *HMRC-UCC OES-IA Under Annex III*, p. T0321, 2010.

[79] [Online]. Available: http://www.novainnovation.com

[80] S. Benelghali, M. E. H. Benbouzid, and J. F. Charpentier, "Generator systems for marine current turbine applications: A comparative study," *IEEE J. Ocean. Eng.*, vol. 37, no. 3, pp. 554–563, Jul. 2012.

[81] M. Liu, W. Li, C. Wang, R. Billinton, and J. Yu, "Reliability evaluation of a tidal power generation system considering tidal current speeds," *IEEE Trans. Power Syst.*, vol. 31, no. 4, pp. 3179–3188, Jul. 2016.

[82] H. H. H. Aly and M. E. El-Hawary, "Comparative study of stability range of proposed PI controllers for tidal current turbine driving DFIG," *Int. J. Renew. Sustain. Energy*, vol. 2, no. 2, pp. 51–62, 2013.

[83] L. E. Myers and A. S. Bahaj, "An experimental investigation simulating flow effects in first generation marine current energy converter arrays," *Renew. Energy*, vol. 37, no. 1, pp. 28–36, Jan. 2012.

[84] L. E. Myers and A. S. Bahaj, "Power output performance characteristics of a horizontal axis marine current turbine," *Renew. Energy*, vol. 31, no. 2, pp. 197–208, Feb. 2006.

[85] M. C. Sousounis, J. K. H. Shek, and M. A. Mueller, "Modelling, control and frequency domain analysis of a tidal current conversion system with onshore converters," *IET Renew. Power Generat.*, vol. 10, no. 2, pp. 158–165, Feb. 2016.

[86] H. H. H. Aly, "Dynamic modeling and control of the tidal current turbine using DFIG and DDPMSG for power system stability analysis," *Int. J. Elect. Power Energy Syst.*, vol. 83, pp. 525–540, Dec. 2016.

[87] J. W. Park, K. W. Lee, and H. J. Lee, "Wide speed operation of a doubly-fed induction generator for tidal current energy," in *Proc. IECON*, 2004, pp. 1333–1338.

[88] S. E. Ben Elghli, M. E. H. Benbouzid, and J. F. Charpentier, "Modelling and control of a marine current turbine-driven doubly fed induction generator," *Renew. Power Generat.*, vol. 4, no. 1, pp. 1–11, 2010.

[89] J. W. Tester *et al.*, "The future of geothermal energy: impact of enhanced geothermal systems (EGS) on the United States in the 21st century," Massachusetts Inst. Technol., Cambridge, MA, USA, Tech. Rep. DE-AC07-05ID14517, 2006.

[90] B. D. Green and R. G. Nix, "Geothermal—The energy under our feet, geothermal resource estimates for the United States," Nat. Renew. Energy Lab., Golden, CO, USA, Tech. Rep. NREL/TP-84040665, Nov. 2006.

[91] *2015 Annual Report, Geothermal Technologies Office*, USDOE EERE, Apr. 2016.

[92] *Technology Roadmap: Geothermal Heat and Power*, International Energy Agency, Jun. 2011.

[93] *2015 Peer Review Report Geothermal Technologies Office*, USDOE EERE, Dec. 2015.

[94] J. Ziagos *et al.*, "A technology roadmap for strategic development of enhanced geothermal systems," in *Proc. 38th Workshop Geothermal Reservoir Eng.*, 2013, pp. 11–113.

[95] *2016 Annual US and Global Geothermal Power Production Report*, Geothermal Energy Assoc., Washington, DC, USA, 2016.

[96] S. K. Sanyal and S. L. Enedy, "Fifty years of power generation at the geysers geothermal field, California—The lessons learned," in *Proc. 36th Workshop Geothermal Reservoir Eng.*, 2011.

[97] D. G. Beyene, "Electrical control and protection system of geothermal power plants," *United Nations Univ. Geothermal Training Program*, no. 13, 2014.

[98] C. Augustine *et al.*, "Renewable electricity futures study: Geothermal energy technologies (Ch 7)," Nat. Renew. Energy Lab., Golden, CO, USA, 2012.

[99] *Geothermal FAQs*, USDOE EERE.

[100] *Levelized Cost and Levelized Avoided Cost of New Generation Resources in the Annual Energy Outlook 2016*, Energy Information Administration, Washington, DC, USA, Aug. 2016.

[101] D. Jovcic, M. Taherbaneh, J. P. Taisne, and S. Nguefeu, "Offshore DC grids as an interconnection of radial systems: Protection and control aspects," *IEEE Trans. Smart Grid*, vol. 6, no. 2, pp. 903–910, Mar. 2015.

[102] M. de Prada, L. Igualada, C. Corchero, O. Gomis-Bellmunt, and A. Sumper, "Hybrid AC-DC offshore wind power plant topology: Optimal design," *IEEE Trans. Power Syst.*, vol. 30, no. 4, pp. 1868–1876, Jul. 2015.

[103] F. Deng and Z. Chen, "Operation and control of a DC-grid offshore wind farm under DC transmission system faults," *IEEE Trans. Power Del.*, vol. 28, no. 3, pp. 1356–1363, Jul. 2013.

[104] C. Meyer, M. Hoing, A. Peterson, and R. W. De Doncker, "Control and design of DC grids for offshore wind farms," *IEEE Trans. Ind. Appl.*, vol. 43, no. 6, pp. 1475–1482, Nov./Dec. 2007.

[105] S. Lauria, M. Schembari, F. Palone, and M. Maccioni, "Very long distance connection of gigawatt- size offshore wind farms: Extra high-voltage AC versus high-voltage DC cost comparison," *IET Renew. Power Generat.*, vol. 10, no. 5, pp. 713–720, 2016.

ABOUT THE AUTHORS

Annette von Jouanne (Fellow, IEEE) received the Ph.D. degree in electrical engineering from Texas A&M University, College Station, TX, USA.

She worked with Toshiba International Industrial Division, Houston, TX, USA. She was a Professor in the School of Electrical Engineering and Computer Science, Oregon State University (OSU), Corvallis, OR, USA, for 22 years, starting in 1995. Her research interests have been in in energy systems, including power electronics and power systems. With a passion for renewables, she initiated the Wave Energy program at OSU in 1998, developing it into an internationally recognized multidisciplinary program. She was also codirector of the Wallace Energy Systems and Renewables Facility (WESRF). In August of 2017, she joined the Department of Electrical & Computer Engineering, Baylor University, Waco, TX, USA.

Dr. von Jouanne has received national recognition for her research and teaching, and she is a registered professional engineer as well as a National Academy of Engineering "Celebrated Woman Engineer."

Ted K. A. Brekken (Senior Member, IEEE) received the B.S., M.S., and Ph.D. degrees from the University of Minnesota, Minneapolis, MN, USA, in 1999, 2002, and 2005, respectively.

He is an Associate Professor in Energy Systems at Oregon State University (OSU), Corvallis, OR, USA. He studied electric vehicle motor design at Postech, Pohang, South Korea, in 1999. He also studied wind turbine control at the Norwegian University of Science and Technology (NTNU), Trondheim, Norway, in 2004–2005, on a Fulbright scholarship. His research interests include control, power electronics and electric drives; specifically digital control techniques applied to renewable energy systems. He is codirector of the Wallace Energy Systems and Renewables Facility (WESRF).

Prof. Brekken is a recipient of the National Science Foundation (NSF) CAREER award.